EDVCATIO PHYSICORVM
SIC ITVR AD ASTRA
QVO NON ASCENDAM ?

# The physics of the spectacular flight of the *Triplaris* samaras

**Celso L. Ladera and Pedro A. Pineda**
*Departamento de Física,*
*Universidad Simón Bolívar,*
*Apdo. 89000, Caracas 1086, Venezuela.*

**E-mail:** clladera@usb.ve

**(**Received 18 June 2009, accepted 14 August 2009)

**Abstract**

*Samaras* are highly specialized forms of "flying" fruits that some species of trees produce for the dispersal of their seeds in their environment. The flight of a samara is always a highly elaborated form of mechanical motion, and an excellent opportunity for application of both Intermediate and Analytical Mechanics to a natural phenomenon. One of the more interesting cases, the passive flight of *Triplaris Caracasana*, which is a combined motion of vertical translation and simultaneous rotation, is presented here. A Newtonian Mechanics model is elaborated, and successfully confirmed, using a variety of different and accurate laboratory measurement techniques including one based on the chopping a laser beam. The motion of the flying samaras is indeed appealing and should be found of great interest for Analytical Mechanics and Fluid Mechanics and as shown here for Intermediate Mechanics courses.

**Keywords:** Classical Mechanics Teaching, Fluid Mechanics, Samaras motion, Newtonian Mechanics.

**Resumen**

Las *samaras* son frutos "voladores", altamente especializados, que algunas especies de árboles producen para lograr dispersarse en su medio ambiente. El vuelo de una samara es siempre una forma muy elaborada de movimiento mecánico, y una excelente oportunidad para la aplicación de la mecánica Analítica o de la Mecánica Intermedia a un fenómeno natural. En este trabajo se presenta uno de los casos más interesantes, el vuelo "pasivo" de la samara del árbol de nombre científico *Triplaris caracasana*, vuelo que es una combinación de traslación vertical y rotación simultanea. Hemos elaborado un modelo basado en Mecánica Newtoniana de dicho vuelo, el cual hemos además validado, y confirmado, mediante la aplicación de diferentes técnicas experimentales, que incluyen una basada en la "interrupción periódica" (el llamado *chopping* en Inglés) del haz de un laser. El movimiento de las samaras voladoras es sin duda atractivo y debe resultar de gran interés para la Mecánica Analítica y la Mecánica de Fluidos y también, como lo demostramos aquí, para la Mecánica Intermedia.

**Palabras clave:** Enseñanza de la Mecánica Clásica, Mecánica de Fluidos, movimiento de la Samara, Mecánica Newtoniana.

**PACS:** 45.40.-f, 45.20.D-, .45.20 dc. **ISSN 1870-9095**

## I. INTRODUCTION

A number tree species, among them *Triplaris caracasana* (vulg. *Palo de María*), *Swetenia mahogany* (vulg. *Caobo de Santo Domingo)* and *Acer macrophyllum* (vulg. *Maple*) [1, 2] have developed rather special ways for dispersing their seeds in their environment. A tree of the venezuelan trade-wind forests, known by its scientific Latin name *Triplaris,* is the subject of the present work. It disperses its seeds by means of a three-winged "flying" fruit, or *samara* (Fig. 1) that rotates quickly in air, while falling to ground from the top of the tree. It is a motion that indeed looks spectacular, particularly when groups of twenty or more samaras are observed simultaneously falling to ground, from the same tree canopy. Dispersal by samaras is indeed very appealing and easily awakes the curiosity of observers. Fig. 1 is a technical drawing of the *Triplaris* samara in vertical position, with its three arched wings inclined at a given angle with respect to the vertical symmetry axis of the samara. The wings of the samara are almost symmetrically displayed (120° apart) about the vertical axis of symmetry of the bulb. The bottom portion of the samara is an ellipsoidal (almost spherical) body, called the bulb, inside of which the seed of the tree is enclosed. *Caobos* and *Maple* trees disperse in similar ways to *Triplaris*, but their samaras are single-winged, not three-winged, and of course much simpler to study. In the outskirts of Caracas, and in mountains and valleys all along the coastline of Venezuela, several of these species of trees, that use winged samaras for their dispersion, are often encountered. But they are not only to be found in Venezuela, they have certainly been found in the southern

coastal forests of Ecuador, and have been even reported in Bolivia and Brazil, south of the Equator. Another remarkable case of passive flying samara is the amazing single-winged samara of the tree of Latin name *Zanonia macrocarpa*, that grows in South-East Asia and the Phillipines Islands. The samara of *Zanonia* practically surfs in air when dispersing. The motion of the "flying" samaras is indeed a subject that many observe since their childhood, but that nonetheless would probably remain a complete mystery for their entire life. Asked by colleagues and students to explain the motion of the *Triplaris* samara, we construct in this work a theoretical model for its "flight" which we have also successfully submitted to experimental tests (Section V).

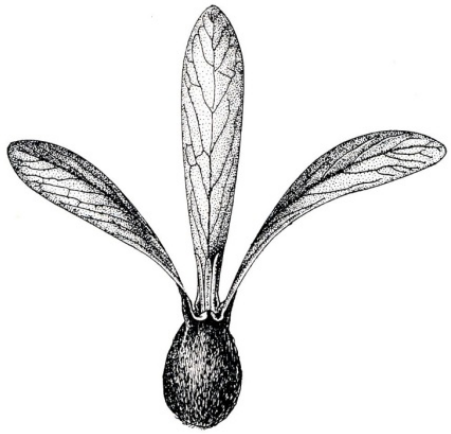

**FIGURE 1**. The samara of *Triplaris Caracasana* in vertical position, as it falls to ground. The three arched and cambered wings are almost equally inclined with respect to the main axis of symmetry. Note the central *nervature* along each wing, and the *bulb* at the bottom, that contains the seed of the tree.

Our model was initially based on analytical mechanics [1] but, as shown below, a simpler formalism based on Newton Second Law may also be used to explain the translational and rotational motions. Below we present both our mathematical model and the experiments that successfully confirm the model predictions. Hopefully, college physics teachers and university lecturers can use our model, and cases similar to *Triplaris*, to enrich their classroom presentations of Newtonian mechanics, and therefore the list of examples of application of physics knowledge to day life. Important science museums across the world have displays of flying samaras.

## II. PHYSICS MODEL OF THE SAMARA

The dispersal flight of a *Triplaris* samara is an appealing natural phenomenon with well-defined physics features, albeit one difficult to explain. The peculiar shape of the samara (Fig. 1), and the possible existence of a cross coupling of *its slow vertical motion* with its *simultaneous rotational motion*, makes it difficult to develop a successful analytical model. When dispersing, *Triplaris* samara is seen to fall slowly to ground, while quickly rotating, as a consequence of its aerodynamics interaction with the air, an interaction in fact driven by the force of gravity, as shall be explained below. As in similar cases of objects falling in air, under the simultaneous action of gravity and some retarding force, we soon noticed – after performing simple kinematics experiments in the laboratory – that there is in fact a final constant translational speed of the samara, the samara *terminal speed*. The main axis of symmetry of the samara practically conserves the vertical orientation all along its descent to ground. This vertical orientation of its axis is conserved even when the samara is being horizontally translated by mild crosswinds. This is simply a consequence of the conservation of angular momentum and the particular morphological design of the samara.

At first sight, however, the motion to ground of a samara would be either uniform, or a descent with a given acceleration. The passive structure of samaras, i.e. the lack of an active engine, or of self-propelling means, suggests that accelerated motion should be considered with care, or at least considered very improbable. The sought analytical model for the samara flight should also clarify the linking between its rotational motion and its translation.

Since a dispersing samara starts its motion to ground from rest, and since it finally reaches a constant terminal translational speed, as experimentally measured in this work (see Section III), it follows that there must be a transient motion regime in which the samara moves with both vertical and angular time-dependent accelerations. The complex morphology of *Triplaris* samaras (Fig. 1), their singular motion, plus the apparently large number of degrees of freedom involved in that motion, suggests the application of Analytical Mechanics, or even advanced Aerodynamics theory, in order to derive a sound physics model for it. The special form of the arched wings (Fig. 1), which in addition are also cambered, and *laterally tilted* a small angle (Fig. 5), suggests the application of sophisticated formalisms used in advanced aerodynamics design [3, 4] such as the Kutta-Zhukovsky formalism or the Navier-Stokes Theorem. As shown below the sought theoretical model can be greatly simplified if some reasonable simplifying assumptions are made. Such assumptions allowed us to simply apply Newton Second Law: $\mathbf{F} = m\mathbf{a}$, where $m$ is the mass of the samara and $\mathbf{a}$ its acceleration. Our physics model is thus based on a set of simplifying assumptions, for instance, when a *Triplaris* samara descends to ground its axis of rotation is seen to remain essentially vertical and coincident with its main symmetry axis all along, therefore our model starts with the assumption that the samara behaves as a rigid body which rotates with respect to such vertical axis. To further simplify the mathematics, the camber and the arching of the wings are also neglected in our model, not so the small lateral *tilt* of the wings. This amounts to a model with three flat, and equally inclined and tilted wings, of constant width $a$. In spite of these seemingly extreme simplifications, our model below has proved to be rather successful.

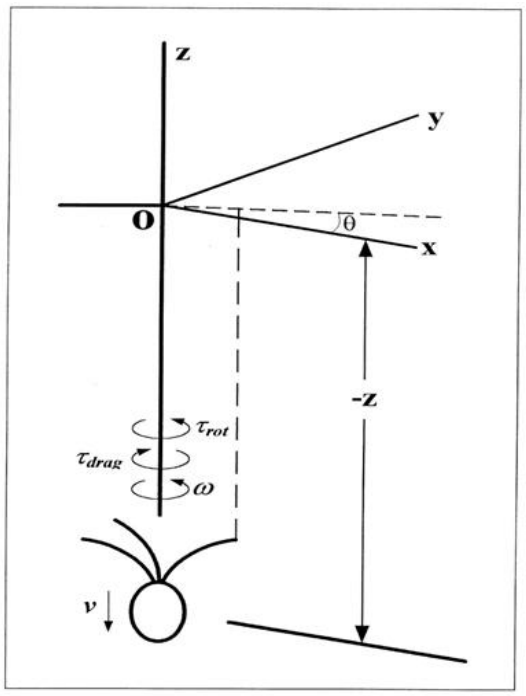


**FIGURE 2.** Natural coordinates used in the physics model of the passively flying samara: $z$ is the vertical position, and $\theta$ is the azimuth angle of rotation measured from the reference x-axis up to the tip of one of the samara wings. Two opposite torques act on the samara: the first torque $\boldsymbol{\tau_{rot}}$ promotes its rotation; the second is the retarding or dragging torque $\boldsymbol{\tau_{drag}}$.

## III. MODEL OF THE VERTICAL MOTION

The natural coordinates for the description of the vertical motion of the *Triplaris* samara (Fig. 2) are the vertical position $z$ measured from the departing position, and the azimuth angle $\theta$ of rotation, measured on a horizontal plane from an arbitrary reference zero-angle horizontal axis to the axis along the tip of one of the samara wings.

The translational motion of the samara is simply along the vertical coordinate $z$. The downward force on the falling samara is its weight $m\boldsymbol{g}$. While falling to ground a vertical force pushes upwards on the samara wings (Fig. 3), it is the vertical component $\boldsymbol{L}_V$ of the so-called *aerodynamic lift vector force* $\boldsymbol{L}$ [1-5]. This force $\boldsymbol{L}$ is simply the sum of the interaction forces of each wing with surrounding air as the samara falls to ground.

Therefore the net vertical force component on the samara is then the difference $mg - L_V$. A straightforward application of Newton Second Newton Law $\boldsymbol{F} = m\,\boldsymbol{a}$ then gives

$$mg - L_V = m\left(\frac{d^2z}{dt^2}\right). \qquad (1)$$

where $d^2z/dt^2$ is the vertical acceleration of the samara.

Let $\rho$ be the air density, $l$ the length of the samara wing, while $\beta$, $\varepsilon$, and $\alpha$ be the angles defined in the wing model depicted in Fig. 3. In the wing reference system, these angles are defined as follows: $\beta$ is the angle of inclination of the flat "wing" with respect to the vertical, $\varepsilon$ denotes the angle of *total deviation* of the *air stream* coming from below when interacting with the inclined wing of the falling samara. Finally, $\alpha$ is the angle that the aerodynamic lift force $\boldsymbol{L}$ forms with the vertical direction (Fig. 3). It is known [1, 3] that the magnitude $L$ of the aerodynamic lift force is proportional to the air density $\rho$, and to the cross-sectional area of the aerodynamic object given in our case by $\pi(l\sin\beta)^2$. This lift is also proportional to the Sine of the deviation angle $\varepsilon$, and finally to the square $v^2(t)$ of the relative vertical speed of the wing with respect to the air. Therefore, the magnitude of the total vertical projection $L_V = L\cos\alpha$ of the aerodynamic lift $\boldsymbol{L}$ (Fig. 3) may be written as:

$$L_V(t) = 3\rho\pi(l\,\sin\,\beta)^2\sin(\varepsilon)\cos(\alpha)v^2(t). \qquad (2)$$

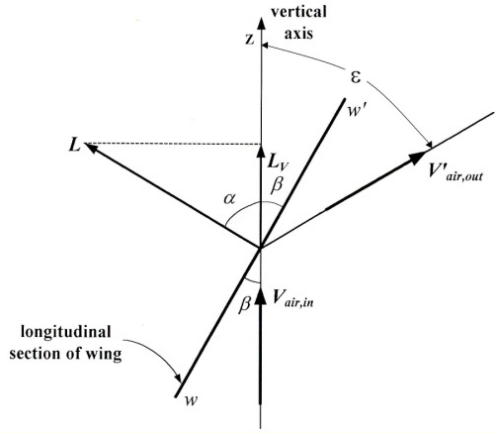


**FIGURE 3.** Physics model of the wing of a *Triplaris* samara. The wing is modelled as a flat slab $ww'$ inclined the angle $\beta$ with respect to the vertical z-axis. **L** is the lift force that the air flowing from below, with velocity $\boldsymbol{v}_{air,in}$ , applies to the wing. The deviation angle of the air flow is denoted $\varepsilon$.

where the factor 3 in the *r.h.s*. of the equation comes from the presence of three wings in the samara. Note that the small change in the magnitude of the velocity of the air-stream as it strikes the wing is also being neglected in our physics model. Only the change of direction of the air-stream *velocity vector* $\boldsymbol{v}$ is considered (Fig. 3). After replacing the expression for the vertical component $L_V$ (equation (2)) into equation (1), and using the definition of the vertical speed $v = dz/dt$, one immediately obtains a differential equation that represents the motion of our model of samara along the vertical axis:

$$\frac{d^2z}{dt^2} + A\left(\frac{dz}{dt}\right)^2 = B. \qquad (3)$$

Fortunately, explicit expressions for the constants $A$ and $B$, can be simply obtained from equations (1) and (2) by simply dividing by the mass $m$. The constant coefficients in equation (3) then become ($g$ is the local *acceleration of gravity*),

$$A = \frac{3\pi\rho\,(l\sin(\beta))^2 sin(\varepsilon)cos(\alpha)}{m}, \quad (4)$$

$$B = g. \quad (5)$$

Ordinary differential equation (3) for the vertical motion is *the first one of a pair of key differential equations* of the present work. Note that Eq. 3 has the form of the well-known *Ricatti* differential equation [7].

This differential equation can be easily solved in *closed* form in just a few steps, and in terms of well-known functions. In effect, let us define:

$$v = \frac{dz}{dt} \quad \Leftrightarrow \quad \frac{dv}{dt} = \frac{d^2z}{dt^2}. \quad (6)$$

Then Eq. (3) for the vertical translation of the modelled samara becomes,

$$\frac{dv}{dt} = B - A\,v^2 \quad \Leftrightarrow \quad \frac{dv}{1-\left(\frac{A}{B}\right)v^2} = Bdt. \quad (7)$$

With the following second change of variables, and its first derivative,

$$\cos(w) = \sqrt{A/_B}\,v \Leftrightarrow \sin(w)\,dw = -\sqrt{A/_B}\,dv, \quad (8)$$

the initial differential Eq.(3) takes a form which can be immediately integrated:

$$\frac{dw}{\sin(w)} = -\sqrt{AB}dt \Leftrightarrow ln\left[tan\left(w/_2\right)\right] = -\sqrt{AB}t + \ln C. \quad (9)$$

Here *C* is a constant whose numerical value is to be found using the known initial conditions: *t = 0 ⇔ v(0) = 0 ⇔ cos w = 0 ⇔ w = π/2*. Hence *C = 1* and the exact solution of the translation motion differential Eq. (3) becomes:

$$\exp\left(-\sqrt{AB}\,t = \tan\left(w/_2\right)\right). \quad (10)$$

To return to the initial variables one simply applies the well-known trigonometric relation

$$tan\left(w/_2\right) = \pm\left(\frac{\sqrt{1-\cos w}}{\sqrt{1+\cos w}}\right). \quad (11)$$

After a few additional algebraic steps one gets the time-dependent function *v(t),* which represents the speed of descent of the samara:

$$v(t) = \sqrt{\frac{B}{A}}tanh\left(\sqrt{AB}\;t\right), \quad (12)$$

which can then be easily integrated in closed form to find the vertical displacement function *z(t)*. The immediate integral formula to find *z(t)* can be found in any standard introductory calculus textbook, or in a handbook [8]. The two required initial conditions are of course the initial position *z(0) = 0*, and the initial speed *v(0) = 0* of the samara for *t=0*. In summary the solutions to Eq. 3 are

$$v(t) = \sqrt{\frac{B}{A}}tanh\left(\sqrt{AB}\;t\right), \quad (13a)$$

$$z(t) = \frac{1}{A}ln\left[cosh\left(\sqrt{AB}\;t\right)\right]. \quad (13b)$$

These functions have been plotted in Fig. 4. From this figure we predict that a *Triplaris* samara descends to ground undergoing an early transient regime of variable acceleration that continuously evolves to a terminal or final uniform motion regime, in only few tenths of a second. This has been confirmed by our experiments (see Section V).

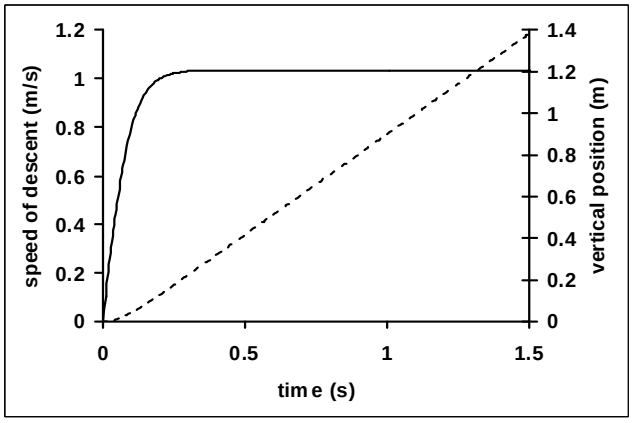


**FIGURE 4.** Speed of descent (continuous line) and the vertical position of a *modelled* samara, as it descends to ground as predicted by the physics model. Note the *non- linear* transient regime at the start of descent, which lasts only about 0.3 s. Note that the predicted terminal speed is close to 1 m/s.

The final uniform motion regime is clearly seen in Fig. 4, it corresponds to the horizontal portion of the plotted continuous line. This terminal speed of the samara can be accurately predicted, or explained, by equation (13a). In effect, the mathematical limit of the function *tanh (t)* as time *t* becomes large, is just 1 (as any calculus textbook shows). This leads to the following exact expression for the *terminal* speed of the modelled samara:

$$v_t = lim_{t\to\infty}v(t) = \sqrt{\frac{B}{A}}\;lim_{t\to\infty}\left(tanh\sqrt{AB}\;t\right) = \ldots\sqrt{\frac{B}{A}}\;.1 = \sqrt{\frac{B}{A}} \quad (14)$$

The non-linear transient motion regime of the falling samara is also clearly represented in the curve for *v(t)* of Fig. 4: it may be seen that such regime starts at *t = 0* and lasts only about 0.25 [s]. After that time the motion becomes uniform, and the speed the terminal speed. The

experimental measurements performed with real samaras have confirmed the validity of our theoretical model. In effect, in the laboratory one observes that a real samara when falling to ground first develops a transient regime of descent, which lasts only a few tenths of a second, and then reaches a terminal speed close to the predicted value $\sqrt{B/A}$ *m/s* (see Section V).

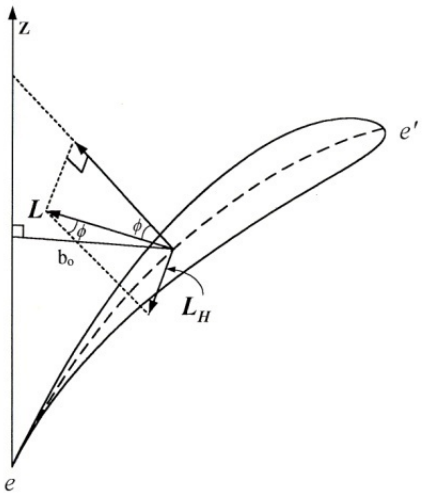


**FIGURE 5.** Horizontal component $\mathbf{L_H}$ (of the lift force **L**). As each wing is *laterally* tilted a small angle $\phi$ the lift force **L** does not lie on the vertical plane defined by the z-axis and the *nervature ee´* of the wing. The small force component $\mathbf{L_H}$ produces the torque that forces the samara into rotation.

## IV. THEORETICAL STUDY OF THE ROTATIONAL MOTION OF A *TRIPLARIS* SAMARA

The relevant coordinate for the rotational motion of the samara is now the azimuth $\theta$ of the tip of a given wing (Fig. 2). Newton Second Law for rotational motion $\tau = I\, d^2\theta/dt^2$ can be applied to the rotation of the falling samara, where $\tau$ is the external torque which forces the samara into rotation, $I$ denotes the moment of inertia of the samara, and $d^2\theta/dt^2$ the *angular acceleration*. Two opposing mechanical torques act on the samara and determine its rotation (see Fig. 2), namely, the *rotational aerodynamic torque* denoted $\boldsymbol{\tau_{rot}}$, and *the drag torque* $\boldsymbol{\tau_{drag}}$, both of which are time-dependent, the first promotes the samara rotation, the second opposes it. Newton Second Law for the samara rotation can thus be written as,

$$\tau_{rot} - \tau_{drag} = I\,\frac{d^2\vartheta}{dt^2} \tag{15}$$

The rotation torque ($\tau_{rot}$) originates from the interaction of the air with the wings as the samara descends. Each wing shows, apart from its vertical inclination $\beta$ a small *lateral inclination*, or tilt, $\phi$ (Fig. 5) which plays the role of *angle of attack* as it rotates, as in the case of a helicopter blade [3, 4, 5]. This lateral inclination means that the reaction force $\boldsymbol{L}$ departs a small tilt angle $\phi$ from the vertical plane that bisects the wing (see Fig. 5). This departure means that a horizontal force component $\boldsymbol{L_H}$, of magnitude $L_H = L_a \sin\phi$, acting on each wing, forces the samara into rotation. These are the horizontal forces that produce the aerodynamic torque $\tau_{rot}$ necessary for the rotation of the samara.

Let us call $b_0$ the mean value of the *arm* of the torque that the force component $\boldsymbol{L_H}$ produces on the samara. This arm is measured from the vertical axis of rotation (Fig 5). The rotational torque, $\boldsymbol{\tau_{rot}}$ on the samara is by definition (*torque = force× arm*):

$$\boldsymbol{\tau_{rot}} = 3(\boldsymbol{b_0} \times \boldsymbol{L_H}) \tag{16}$$

where again the factor 3 comes from the existence of three wings in the samara and $\mathbf{L_H}$ is orthogonal to $\mathbf{b_0}$ .

Moreover the horizontal component $L_H$ of the lift force can be shown (see *Appendix A*) to be given by,

$$L_H = L(t)\sin(\phi) = \pi\rho\,(l\,sin\beta)^2 \sin(\varepsilon)\sin(\phi)\,v(t)^2, \tag{17}$$

and $\tau_{rot}$ can then be found using Eq. (16): $\tau_{rot}=3b_0 L_H$.

It now only remains to find an expression for the second aerodynamic torque on the samara, which is the *dragging torque* $\boldsymbol{\tau_{drag}}$. This second torque arises from the air drag on the upper surfaces of the wings as the samara rotates. After a simple integration of the drag force along the top of a single wing (see *Appendix B*) one find this drag torque to be given by Eq. (27):

$$\tau_{drag} = \left[\tfrac{3}{8} C_d \rho (a l^4) sin^3(\beta)\right] \omega^2(t), \tag{18}$$

where again $a$ denotes the wing width, $C_d$ is the dimensionless *drag coefficient*, and finally $\omega = d\theta/dt$ is the rotational angular speed of the samara.

Replacing expressions ((16) - (18)) into equation (15) and after division by the moment of inertia $I$, one gets the *second key differential equation* of our physical model,

$$\frac{d^2\theta}{dt^2} = E v^2(t) - D\left(\frac{d\theta}{dt}\right)^2, \tag{19}$$

where the constant $D$ is just the drag torque $\tau_{drag}$ given by Eq. (18) divided by the moment of inertia $I$, that is

$$D = \frac{3}{8I} C_d \rho (l^4 a) sin^3(\beta), \tag{20}$$

while the constant $E$, related to the aerodynamic torque $\boldsymbol{\tau_{rot}}$ that favours the rotation, is found using Eqs. (16), (17), (19) and *Appendix A*, and is given by:

$$E = \frac{3\pi}{I} \rho (l sin\beta)^2 b_0 \sin(\phi)\sin(\varepsilon). \tag{21}$$

Note that the first term in the right-hand side of the rotational motion differential equation (19) is quadratic on

the angular speed $d\theta/dt$. It is a non-linear differential equation that cannot be integrated in closed form [7]. A different procedure, in fact a numerical integration, may be used to solve it. Constants values $D$ and $E$ are also required. Simple measurements on our field collected sample specimens of samaras gave the average values of required parametres to evaluate the two constants $D$ and $E$ in equations (20) and (21) (wing length $l = 37\ mm$, wing width $a = 6\ mm$, inclination $\beta = 35°$). The density of humid air, at the local atmospheric pressure of 89311 Pa (*i.e. 67 cm Hg*) and at a local temperature of $26°\ C$, is approximately $\rho = 1.05\ kg/m^3$ [8]. The mean value of the torque arm $b_0 = 12\ mm$, is determined from direct measurements on the collected sample of samaras.

The value of the *drag coefficient* $C_d$ for a samara wing proved to be a difficult constant to find. In principle it should be experimentally determined in a wind tunnel, a facility not available to us. As a reference, the drag coefficient for the wing of a *locust* insect is 0.1. A rough estimate of the samara surfaces drag constant $C_d$ could be obtained in a straightforward way by applying the principle of Conservation of Energy to the samara motion, *i.e.* equating the initial gravitational energy of the samara to the sum of its kinetic energy, rotational kinetic energy, and using an estimate for the drag dissipated energy (the total kinetic energy of the air stream about the samara has also to be included).

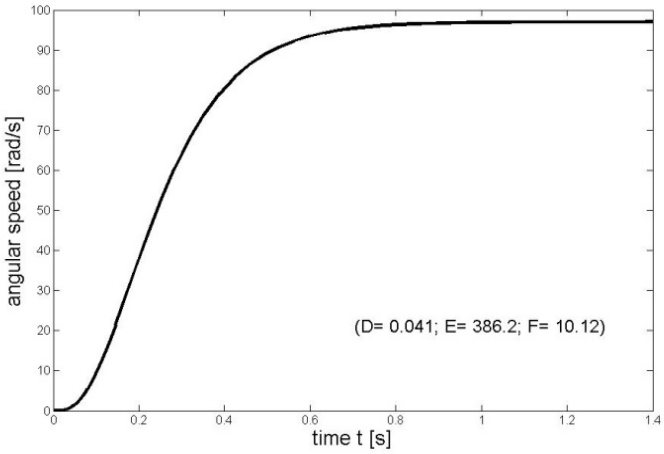


**FIGURE 6.** Predicted angular speed of a samara (its physics model) as a function of time. The terminal angular speed is close to *98.4 rad/s* (about 16 R.P.S). Note the non-linear transient regime that lasts for about 0.85s.

This rough calculation gave us the order of magnitude for the drag coefficient $C_d \sim 10^{-1}$. A search of the literature gave us the required information [9] for the small angle of attack $\phi \approx 2°$ of the samara and $C_d \approx 0.2$, the value used in this work.

The moment of inertia $I$ of the samara, which appears in equations (9), (14) and (15), remains to be determined. An exact value of this parameter is out of the question. Our model of samara consists of a small spherical bulb with three equally inclined flat plates emerging from its top (Fig. 1). Its moment of inertia can then be approximately obtained using tabulated expressions for the moment of inertia of a sphere and 3 equally inclined flat wings [10]. The result obtained is $I \approx 4.3\times 10^{-9}\ kg\ m^2$. With the two constants $D$, $E$ already known, it only remains to solve the motion equation (13) to explain how the *Triplaris* samara rotates. The variable speed $v(t)$ function is required in (19); fortunately it was already obtained in our study of the vertical translation of the samara (see equation (13a)). When all the relevant constants of the samara were introduced into equation (21) the constant value $E = 3.862\times 10^2\ m^{-2}$ was found. The constant $D = 4.07\times 10^{-2}$ was also found.

The *numerical algorithm* of Runge and Kutta [11] was used, with the known initial conditions $\omega(0) = 0$ for $t = 0$, to solve the non-linear differential equation (19). The angular speed function $\omega(t)$ and the angular position $\theta(t)$ of the samara were then obtained. The angular speed function $\omega(t)$ predicted by the model is plotted in Fig. 6. Note that a terminal, or final, angular speed $\omega_t \approx 98.4\ rad/s$ (equivalent to about 16 turns per second) is predicted for large values of time $t$. As can be noticed in Fig. 6 this terminal angular speed is reached about $0.85\ s$ after the samara begins its fall to ground. We must also mention that there are readily available commercial software that can be used to solve numerically the two key differential equations of motion Eqs. (3) and (19), of the samara.

## V. EXPERIMENTS AND RESULTS

Controlled experiments with a real samara in its natural environment are difficult to perform. Wind turbulences, the height (≈20 *m*) of the *Triplaris* canopy, and the ferocious ants that every *Triplaris* tree happens to host, forbid systematic studies in the field. Our initial, simple laboratory experiments (allowing a real samara to fall from rest) showed that, at least in quiet air, the path of the centre of mass of a given samara keeps sufficiently close to a vertical line, while it falls to ground.

A set of preliminary kinematics experiment, using a chronometer and a vertical five-metre long tape were performed to measure the times for a falling and rotating samara to reach previously marked vertical positions. The preliminary results, although not very accurate, gave hints that a small constant terminal vertical speed is soon achieved by the samara, and also hinted that an early transient regime of motion does exist. A second set of more accurate experiments were performed using *ultrasonic ranging.* This second technique is a very accurate way for localizing the samara as it falls vertically.

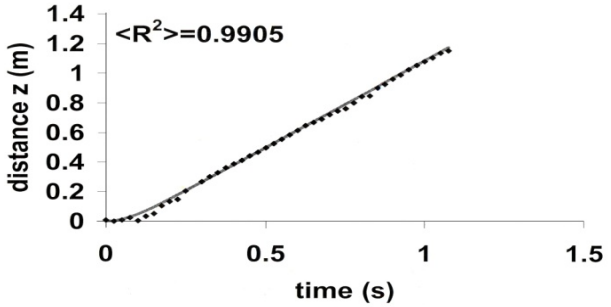


**FIGURE 7.** The plotted data points (dots) are the experimentally measured vertical positions of a real samara in its retarded fall to ground. The continuous curve is the predicted vertical displacement given by our physics model. Note the excellent agreement and the short non-linear transient regime ($R^2$ is the correlation).

We placed an ultrasound-ranging sensor on the floor, interfaced it to a personal computer, and different samaras were allowed to fall from 3-4 m above the sensor, and along the vertical through the sensor. The dotted line in Fig. 7 represents a typical experimental result for the vertical position of a real samara measured using this ultrasonic ranging technique, while the continuous curve is the vertical displacement function *z(t)* given by the theoretical model of samara, Eq. (13b).

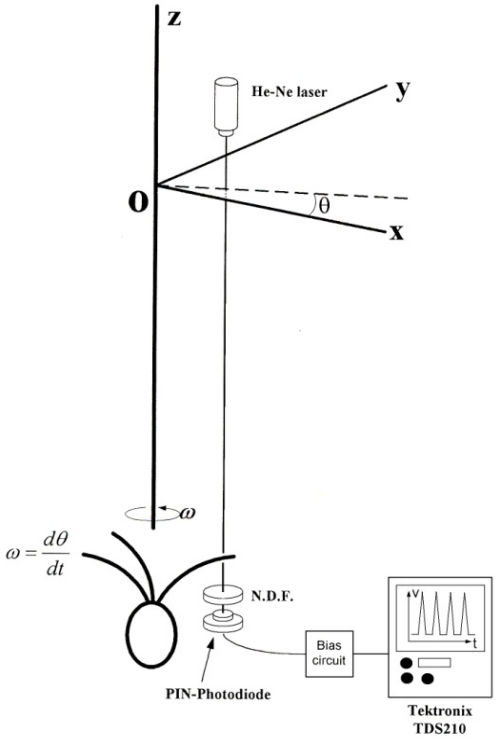


**FIGURE 8.** *Optical beam shopping method* used for the measurement of the terminal angular speed ω of a *real* samara. A He-Ne laser beam is set along a vertical and detected, after attenuation by a neutral density filter NDF, by a reverse-biased PIN photodiode. The rotating wings of the samara chop the beam and the photo signal generated is displayed and stored in a digital oscilloscope.

Recall that the constant *B* (in Eqs. (13a) and (13b)) is simply the local gravitational acceleration ($g = 9.78\ m/s^2$ in the outskirts of Caracas). Note the good agreement between the predictions of our theoretical model and the experimental data (Fig. 7). As predicted the terminal speed of a real samara is about *1 m/s*, as given by the slope of the straight portion of the curve in Fig. 7.

The terminal *angular speed* ω of the samara was measured using two procedures, firstly using an electronic stroboscope, and secondly using a method based on the shopping of a laser beam. The laser beam chopping method has greater accuracy and is far easier to apply (Fig. 8) than the stroboscope method, it relies on the samara descending close to a vertical line.

The results obtained with both methods are fortunately consistent and, what is better, the same. The optical beam chopping technique is very reliable and gives data that can be easily processed and therefore it is the one we present it here (see Fig. 8). A 2mW He-Ne laser beam is aligned vertically in the laboratory and a reverse-biased PIN photodiode is placed on the floor at the point where the laser beam strikes the floor. A neutral density filter (NDF) is used to attenuate the laser beam to avoid saturating the photodiode. As the samara falls to ground in close proximity to the vertical laser beam, its 3 wings shop the beam. The photodiode circuit then gives a periodic pulsed signal that is displayed (Fig. 9) and registered against time in a digital oscilloscope (Tektronik TDS-210 [R.M.]).

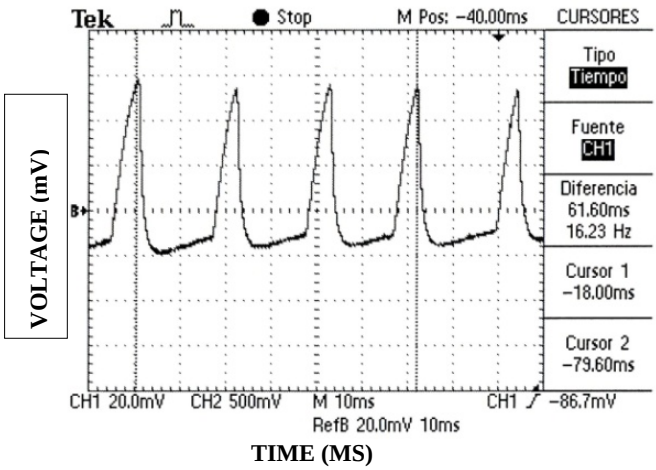


**FIGURE 9.** Terminal angular speed of a real samara measured using our *optical beam chopping method*. The voltage signal generated by a photodiode is displayed, and stored, in a digital oscilloscope and the frequency of rotation of the samara (16.23 Hz) is directly obtained using the two *time cursors* of the oscilloscope menu (here set at peaks 1 and 4).

Fig. 9 shows a typical oscilloscope trace obtained with this optical chopping technique. Note that one can directly measure the time intervals between successive signal peaks (when the laser beam manages to pass towards the photo-detector, in between the rotating wings). The time intervals between such signal peaks are of course a third of

the samara period of rotation, and give directly the temporal frequency of rotation. From such oscilloscope traces the measured mean terminal angular speed, for a sample of 15 samaras, was obtained $\omega_t = 100.2 \pm 1.4$ *rad/s*, a value that confirms the validity of our theoretical model. In effect our model, for the real samara used in that experiment, predicts a value $\omega_t \approx 98.4$ *Hz*, very close enough to the measured one (only about 2 % error). In passing, note the excellent quality of the experimental results given by the optical chopping technique.

## VI. DISCUSSION AND CONCLUSIONS

*Triplaris* samaras perform a motion that apparently can be described as a simple superposition of independent rotation and translation. Instead, we found in this work that the rotation is induced by an aerodynamic torque forced on the laterally inclined wings by interaction with the surrounding air, as the samara travels to ground. The small lateral inclination, or tilt $\phi$ (Fig. 5), produces small horizontal forces (horizontal components of the lift force $\boldsymbol{L}$ on the wings) that generate the rotational torque.

This cross-coupling between the vertical translation and the rotation is the key to the dispersal strategy of the samara: *it induces the final long-lasting terminal regime, which then favours the horizontal transport, i.e. the dispersal of the samara by transverse winds.*

We found that the samara vertical translational motion is separated into two different regimes, a short non-linear initial *transient*, and a final uniform *terminal* regime. The terminal vertical speed has been experimentally measured, with good accuracy and precision. Starting with a set of basic assumptions, and with the application of well-known elementary physics, a theoretical model has been established. This model is capable of predicting the non-linear motion as well as the terminal regime of the samara.

A samara finally reaches ground with a mean speed close to *1 m/s*, the actual value depending upon its physical parameters (mass, wing inclination, and the like). The model also predicts a terminal angular speed $\omega_t$ close to *98.5 rad/s*. A special experimental method (the *optical beam chopping*) was developed by us to measure accurately the terminal angular rotation speed of the samaras. The experiments with a sample of samaras gave a mean angular speed $\langle\omega_t\rangle = 100.1$ *Hz*, close enough to our theoretical prediction (only about 1.6% error).

In Fig. 7 small "oscillating" departures, similar to the *librations* of an axis-symmetric conical spacecraft [12], are observed with respect to the theoretical curve. They are to be explained by the small wobbling of a real samara as it falls to ground. Recall we made the assumption that the samara falls to ground with its symmetry axis exactly along a vertical, while a real samara axis can wobble a bit, as spacecrafts do. A refined model must account for these small *librations* of the samara axis as it falls. Finally, during the present work we discovered an unexpected *dimorphism* attribute, or symmetry-breaking, of the *Triplaris* samaras: some samaras behave as *right-hand airscrews*, and develop upward spin (i.e. angular velocity oriented upward), others are *left-hand airscrews* and develop downward spin. The *spin* orientations of samaras, and the role if any, that small asymmetries of the samaras (in wing size, angular separation, different wing tilts and the like) have in the dispersal flight, deserve further investigation.

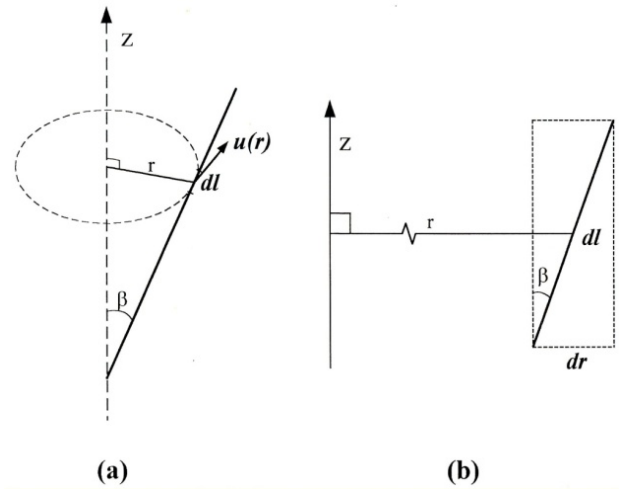


**FIGURE 10. (a)** Tangential speed u(r) of a small element ***dl*** of wing that rotates with respect the vertical ***z*** – axis. The radial distance is *r* and $\beta$ is the inclination angle of the wing. **(b)** *dl* and *dr* are related by $dr = dl \sin \beta$.

## ACKNOWLEDGEMENTS

We acknowledge Mr. Washington M. Marín help, a member of our staff, for his collaboration to improve the figures of the manuscript.

## REFERENCES

[1] Ladera, C. L., Pineda, P. A. and Alcalá, G., *Modelo analítico del vuelo de dispersión del aquenio de Triplaris caracasana,* Ciencia **8**, 285-303 (2000).
[2] Schlichting, H, Ucke, C., *Der Flug des geflügelten Samens*, Physik **25**, 79-80 (1994).
[3] Waltham, C., *Flight without Bernoulli*, Physics Teacher **36**, 457-462 (1998).
[4] Clancy, L. J., *Aerodynamics,* (Pitman Pub. Ltd., London, 1975).
[5] Streeter, V. L. and Wylie, E. B., *Fluid Dynamics*, 8th. ed., (McGraw-Hill, New York, 1986) pp. 243-277.
[6] Rosen, A. and Seter, D., *Vertical Autorotation of a Single-Winged Sámara,* Transactions of the A.S.M.E. **58**, 1064-1071 (1991).
[7] Davis, H. T., *Introduction to Nonlinear Differential Equations,* (Dover, New York, 1962) pp. 57-76.
[8] Hodgman, C. D, Weast, R. C, Shankland, R. S. and Selby, S. M., *Handbook of Chemistry and Physics*, 44th. ed., (The Chemical Rubber Pub. Co., Cleveland, 1962) pp. 2200-2204.

[9] Vogel, S., *Life's devices: The Physical World of Animals and Plants, (*Princeton University Press, Princeton, 1988) pp. 130-157.
[10] Hudson, R. G., *The Engineer's Handbook*, 2nd. ed. (Wiley, New York, 1961) pp. 87-93.
[11] Pang, T., *An Introduction to Computational Physics*, (Cambridge University Pr., Cambridge, 1997) pp. 60-67.
[12] Fortescue, P. W., Stark, J. and Swinerd, G. Eds., *Spacecraft System Engineering*, 3rd ed. (U.K.:Wiley, Southampton, 2002) Ch. 9.

## APPENDIX

### A. EVALUATION OF THE AERODYNAMIC TORQUE OF ROTATION

The aerodynamic torque of rotation on the samara originates from the aerodynamic lift force $\boldsymbol{L}$ on its wings**.** As explained in Section 2 the wing of a samara shows a small lateral tilt $\phi$ (Fig. 5). Therefore the wing plane forms an angle $(90+\phi)^\circ$ with respect to a vertical plane drawn through the wing central *nervature* (Fig. 1). Because of this tilt the force vector $\boldsymbol{L}$ crosses (do not intersect) the vertical rotation axis of the samara, and therefore there exists a horizontal component $\boldsymbol{L_H}$ (Fig. 5) that crosses the vertical axis orthogonally. The magnitude of this force component is of course (Fig. 5) given by $L_H = L \sin\phi$. It is well-known [3, 11] that the magnitude $L$ of the aerodynamic lift force on a wing is proportional to the air density ρ, to the square of the relative speed $v$ with respect to air, and to the wing cross-section. Therefore in the present case $L$ may be written as:

$$L = 3\,\pi\,\rho\,\left(l\,sin(\beta)\right)^2\,sin(\varepsilon)\,v^2(t). \qquad (22)$$

The component $L_H = L \sin\phi$ can then be found and so the product $b_0 L_H$ (see Fig. 5) finally gives the desired rotational torque Eq. (16), on the wings.

### B. EVALUATION OF THE DRAG TORQUE

The drag between the air and the surfaces of the rotating wings produces the drag torque. This force is proportional [3, 4] to the air density $\rho$, to the area of the surface over which the air flows, and to the square $u^2$ of the relative *air/surface* speed, the proportionality constant being the drag coefficient $C_d$. Recall that $l$ is the length of the assumed flat wing in our model, and $a$ is its width in Fig. (10a). Consider the differential element of wing $dl$ (Fig.10a) whose radial distance to the axis of rotation is $r$. The infinitesimal torque of the wing differential element of area $adl$ is then

$$d\tau_{drag} = r\left[\frac{C_d}{2}\right]\rho(adl)u^2(r). \qquad (23)$$

The tangential speed of this wing differential element is simply $u(r) = \omega\, r$, where $\omega$ is the angular speed of the samara. The length differential element $dl$ is (Fig. 10b)

$$dl = \frac{dr}{\sin(\beta)}. \qquad (24)$$

Replacing this equation in the previous one, the following expression of the differential drag torque ensues,

$$d\tau_{drag}(t) = \frac{3C_d}{2\sin(\beta)}\rho a\omega^2(t)r^3dr. \qquad (25)$$

The total drag torque on the *three* wings of our model of samara is obtained by integrating along the whole wing, that is integrating between the limits $0$ and $l \sin\beta$:

$$\tau_d(t) = \frac{3}{2}\frac{C_d}{\sin(\beta)}\rho a\omega^2(t)\int_0^{l\sin(\beta)} r^3dr. \qquad (26)$$

The integral in the right hand side is immediate and the result gives Eq. (18) above,

$$\tau_{drag}(t) = [\frac{3}{8}C_d\rho a\, l^4\sin^3(\beta)]\,\omega^2(t). \qquad (27)$$